Geoderma 355 (2019) 113899

Contents lists available at ScienceDirect

Geoderma

journal homepage: www.elsevier.com/locate/geoderma

Composition and superposition of alluvial deposits drive macro-biological soil engineering and organic matter dynamics in floodplains

A. Schomburg[a,b,*], D. Sebag[c,d], P. Turberg[e,f], E.P. Verrecchia[c], C. Guenat[e,f], P. Brunner[b], T. Adatte[c], R. Schlaepfer[e,f], R.C. Le Bayon[a]

[a] Functional Ecology Laboratory, Institute of Biology, University of Neuchâtel, Switzerland
[b] Center for Hydrogeology and Geothermics (CHYN), University of Neuchâtel, Switzerland
[c] Institute of Earth Surface Dynamics, Geopolis, University of Lausanne, Switzerland
[d] Normandie University, UNIROUEN, UNICAEN, CNRS, M2C, 76000 Rouen, France
[e] Laboratory of Ecological Systems – ECOS-EPFL, Ecole Polytechnique Fédérale de Lausanne (EPFL), Switzerland
[f] WSL Swiss Federal Institute for Forest, Snow and Landscape Research, Site Lausanne, Switzerland

ARTICLE INFO

Handling Editor: Yvan Capowiez

ABSTRACT

Soil structure formation in alluvial soils is a fundamental process in near-natural floodplains. A stable soil structure is essential for many ecosystem services and helps to prevent river bank erosion. Plants and earthworms are successful soil engineering organisms that improve the soil structural stability through the incorporation of mineral and organic matter into soil aggregates. However, the heterogeneous succession of different textured mineral and buried organic matter layers could impede the development of a stable soil structure. Our study aims at improving the current understanding of soil structure formation and organic matter dynamics in near natural alluvial soils. We investigate the effects of soil engineering organisms, the composition, and the superimposition of different alluvial deposits on the structuration patterns, the aggregate stability, and organic matter dynamics in *in vitro* soil columns, representing sediment deposition processes in alluvial soils. Two successions of three different deposits, silt–buried litter–sand, and the inverse, were set up in mesocosms and allocated to four different treatments, i.e. plants, earthworms, plants + earthworms, and a control. X-ray computed tomography was used to identify structuration patterns generated by ecosystem engineers, i.e. plant root galleries and earthworm tunnels. Organic matter dynamics in macro-aggregates were investigated by Rock-Eval pyrolysis. Plant roots only extended in the top layers, whereas earthworms preferentially selected the buried litter and the silt layers. Soil structural stability measured via water stable aggregates (%WSA) increased in the presence of plants and in aggregates recovered from the buried litter layer. Organic matter dynamics were controlled by a complex interplay between the type of engineer, the composition (silt, sand, buried litter) and the succession of the deposits in the mesocosm. Our results indicate that the progress and efficiency of soil structure formation in alluvial soils strongly depends on the textural sequences of alluvial deposits.

1. Introduction

Soils of near natural floodplains constitute an important pillar to the preservation of biodiversity in floodplain ecosystems. At small spatial scales, floodplain soils differ considerably in their physicochemical properties, forming a large variety of terrestrial habitats (Malmqvist and Rundle, 2002). Besides, they fulfil a broad range of ecosystem services, ranging from carbon sequestration, nutrient and pollutant cycling, up to flood and erosion control (Diaz-Zorita et al., 2002; Acreman et al., 2003; Bronik and Lal, 2005). Focusing on pedogenesis, floodplain soils, such as Fluvisols or Fluvic Arenosols (IUSS Working Group WRB, 2015), are composed of different alluvial sediments that are superimposed due to recurring flood events (Nanson and Croke, 1992; Marriot, 1998). Alluvial deposits may differ considerably in their thickness and composition, e.g. in their texture, as well as in their organic matter (OM) content and bulk chemistry, depending on the flood magnitude and the sediment origin (De Vivo et al., 2001; Coppola et al., 2010). Soil physicochemical parameters can thus abruptly change in a soil profile, whenever a previous topsoil horizon is overlaid by a more recent alluvial deposit (Kercheva et al., 2017). Moreover, litter overtopping topsoil horizons can be buried before being mixed with the soil matrix depending on the season, OM type and decomposition rates, and

* Corresponding author at: Functional Ecology Laboratory, Institute of Biology, University of Neuchâtel, Switzerland.
E-mail address: andreas.schomburg@unine.ch (A. Schomburg).

https://doi.org/10.1016/j.geoderma.2019.113899
Received 8 October 2018; Received in revised form 21 July 2019; Accepted 1 August 2019
Available online 20 August 2019

soil biota activity. Consequently, strong alluvial dynamics with regular flood events over a year may either wash away or leave sediment behind thus completely resetting the pedogenesis (Malmqvist and Rundle, 2002). The stabilisation of floodplain soils is then often hindered and mediated by a complex interplay between soil physicochemical parameters, soil engineering organisms, and surface-water–groundwater dynamics (Guenat et al., 1999; Plum and Filser, 2005; Bullinger-Weber et al., 2007, 2012; Fournier et al., 2012; Schomburg et al., 2018b, 2019). The vegetation composition and ecosystem services in floodplains are positively affected by stable conditions in the soil, which can be promoted by its structural stability and by the extension of the soils' macro-porous system (Bronik and Lal, 2005).

Plants and earthworms are among the most successful soil engineering organisms at the macro-biological scale in temperate ecosystems (Lavelle et al., 1997; Tanner, 2001; Blouin et al., 2013; Le Bayon et al., 2017). By mixing mineral particles and soil organic matter (SOM), they form soil macro-aggregates, which significantly improve soil's structural stability (Brown et al., 2000; Six et al., 2002; Kong and Six, 2010). Plants physically entangle mineral and organic soil particles through rooting and releasing root exudates, which act as a glue or stimulate rhizobacteria (Degens et al., 1994; Angers and Caron, 1998; Czarnes et al., 2000). Earthworms agglutinate soil particles along burrow walls or in casts, as they select organic and mineral components and enrich ingested material with mucus and saliva produced in their digestive system (Blanchart et al., 1997; Brown et al., 2000; Lavelle and Spain, 2001; Curry and Schmidt, 2007). Both plants and earthworms also have great potential for improving the structural stability in floodplain soils, as some species rapidly colonise young soils and tolerate periodic flood events (Gurnell and Petts, 2002, 2006; Thonon and Klok, 2007; Le Bayon et al., 2013, 2017; Schomburg et al., 2018b, 2019).

However, soil structuration patterns (i.e. the way to form aggregates and pore space) created through plant rooting and through earthworms' burrowing and casting activities are still rarely investigated and poorly understood in floodplain soils. Secondly, the unique development of floodplain soil layers has never been considered in the analysis of soil structure formation. Specifically, the combined consideration of the superposition of several alluvial deposits of different texture in addition to the influence of buried litter is unique to our study. In the field, such structuration patterns are difficult to appraise due to spatial heterogeneity of superimposed alluvial deposits. Hence, standardising these parameters in the laboratory using mesocosms may be a useful way to investigate soil structuration patterns through plant rooting and earthworm activities. Root galleries and earthworm tunnels in micro- and mesocosms can be visualised and analysed using X-ray computed tomography (X-ray CT; Pierret et al., 1999, 2002; Capowiez et al., 2011, 2015; Amossé et al., 2015; Schomburg et al., 2019). X-ray CT is a non-destructive tool used to create a 3D structure of a scanned matrix, and thus, analyses its macro-porous network (Helliwell et al., 2013; Turberg et al., 2014). By doing so, X-ray CT has emerged as a contemporary method to indirectly assess soil structure formation (Vogel et al., 2002; Vervoort and Cattle, 2003; Lin et al., 2005). Similarly to structuration patterns, OM dynamics and in particular the mechanisms of its mixing with mineral particles are strongly controlled by the heterogeneous layout of floodplain soils. The origin of OM in soil aggregates can however be distinguished through the analysis of its thermal stability by the way of indices representing immature OM (I-index) and OM thermal stability (R-index) (Albrecht et al., 2015; Sebag et al., 2016; Matteodo et al., 2018; Schomburg et al., 2018a).

As floodplains are essential components of many important ecosystem services, such as water regulation (Acreman et al., 2003) and are prone to riverbank erosion (Diaz-Zorita et al., 2002), understanding the processes of soil stabilisation is crucial. In the present study, our main hypothesis is that the type of soil engineer, the composition of the deposits (sediment and litter) and how they are superimposed strongly control the structuration patterns and the structural stability of soil aggregates. Hence, we investigate the combined effects of different alluvial deposits, their superimposition, and also the role of soil engineering organisms on the formation of soil aggregates and in OM dynamics. For this purpose, we use a mesocosm approach and simulate a natural floodplain soil through the superposition of two alluvial sediments strongly differing in their texture and separated by a layer of buried litter material. We expect that a finer soil texture (e.g. silt) would overall favour structuring processes by plants and earthworms and that a buried litter layer would be a catalyst for the formation of soil aggregates.

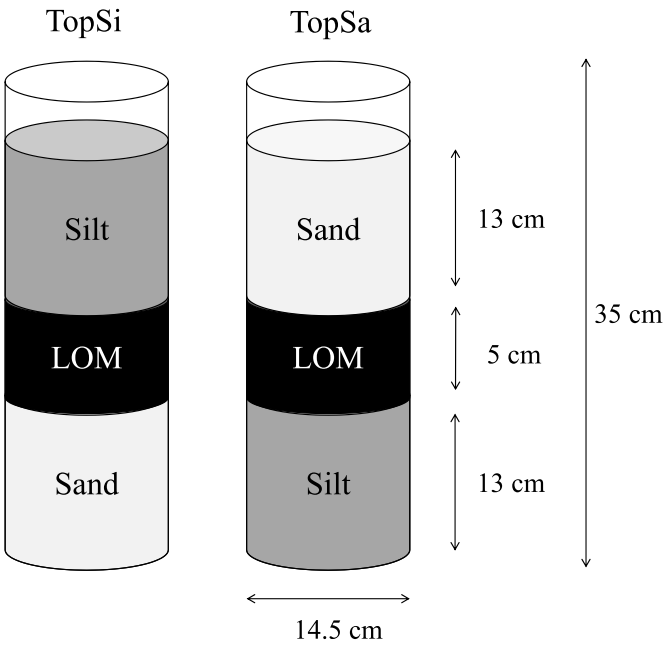

Fig. 1. The two mesocosms' experimental designs with silt (silt.top), overlying an organic matter layer (LOM) and a sand layer (sand.bottom) (TopSi) and sand (sand.top), overlying an organic matter layer (LOM) and a silt layer (silt.-bottom) (TopSa).

2. Material and methods

2.1. Experimental design

To test our hypothesis, we set up an experimental *invitro* mesocosm design based on the one proposed by Schomburg et al. (2018a). Two alluvial sediment deposits (a silty and a sandy one) were superposed and separated by a layer of litter material (LOM layer) following two different superimpositions (Fig. 1): i) the silty sediment overtopping the sandy one (TopSi configuration with silt.top, LOM, sand.bottom) and ii) vice versa (TopSa configuration with sand.top, LOM, silt.bottom). Both configurations were allocated to four different treatments with five replicates each: i) the plant treatment (P), ii) the earthworm treatment (EW), iii) the combined plant and earthworm treatment (P + EW), and iv) the control (NT) ($2 \times 4 \times 5 = 40$ mesocosms in total). This experimental design generated two different layouts for the data analysis: i) a one-factor design for the data that was available at the mesocosm level (plant biomass and weight gain of earthworms, see Section 2.4); the studied factor was the “treatment” with four levels (P, EW, P + EW, NT); ii) a split-plot design for the data measured at the split plot level; the main unit factor was represented by the “treatments” and the split-plot factors were the three kinds of material (silt, sand, LOM) within the mesocosms. In addition, the position of each material within the mesocosm was defined by its “layer”: silt.top, silt.bottom, sand.top, sand.bottom, LOM (which is always the second layer; Fig. 1). Using this definition, the split-plot factor had five levels. The response variables

Table 1
Initial soil physicochemical parameters measured in silty and sandy alluvial sediments before starting the incubation experiment. Grain size distributions were obtained using a LS 13 320 Laser Diffraction Particle Size Analyzer equipped with an APS Auto Prep Station (Beckman Coulter); pH values were measured using a combined pH meter/conductometer (914 pH Meter/conductometer, Metrohm, Herisau) with a soil/water ratio of 1:2.5; TOC contents are calculated from Rock-Eval pyrolysis and total carbonate contents were obtained using a Bernard Calcimeter described by Vatan (1967).

Soil parameter	Silty sediment	Sandy sediment
Silt content (%)	56.00	4.50
Sand content (%)	34.50	92.50
Clay content (%)	9.50	3.00
pH_{water}	7.45	8.25
TOC content (%)	1.48	0.32
Total carbonate content (%)	37.00	30.00

measured at the split-plot levels were the total segment length analysed by X-ray computed tomography (see Section 2.3), the percentage of water-stable macro-aggregates (%WSA, see Section 2.4), and the R-index for OM dynamics (see Section 2.5).

2.2. Mesocosm set up

Mesocosms were set up in cylindical PVC tubes of 35 cm in height and 14.5 cm in diameter. Sand, silt, as well as litter and small branches of willow trees (*Salix viminalis*) for the LOM layer were sampled in the willow bush area (Fournier et al., 2012) in the restored section of the Thur River in Niederneunforn (8°77′12″ E, 47°59′10″ N), Thurgau Canton, Switzerland. Both sediments were recent alluvial deposits of a (i) Calcaric Fluvisol and a (ii) Calcaric Fluvic Arenosol (IUSS Working Group WRB, 2015). Soil physicochemical parameters and the methods used for their respective analysis are listed in Table 1. Before filling the tubes, sediments and litter material were dried at 40 °C for 72 h in order to preserve the SOM fraction. Sediments were sieved mechanically at 1 mm using a vibrating sieving apparatus. The fraction between 1 and 2 mm was neglected in order to destroy pre-existing macro-aggregates and to remove the coarse sand fraction that may cause intestinal damage to earthworms' digestive tracts (Shipitalo and Protz, 1988). Sampling of ecosystem engineers and preparation of PVC tubes were performed similar to the design presented by Schomburg et al. (2018a). Each PVC tube was filled up with 2.5 kg of both sediments, which were mixed with 1.5 g of dried and shredded catgrass (*Cyperus zumula*) in order to supply food to earthworms during the experiment. The first sediment was filled stepwise into the tube and rewetted to field capacity after each 2 cm of filling. This sediment was superposed by 10 g of willow tree branches and leaves of similar size corresponding to 5 cm of filling height. This layer was again covered by the other sediment and vice versa.

The endogeic earthworm *Allolobophora chlorotica* and the canary grass *Phalaris arundinacea* were chosen as soil engineers. Both of them were the most abundant species at the Thur River floodplain and thus representative to analyse soil structure formation in alluvial soils. For the plant treatment (P), a seedling of *Phalaris arundinacea* (8–10 g initial weight) was planted during sediment filling. For the earthworm treatment (EW), five adult individuals of the endogeic *Allolobophora chlorotica*, sampled one day before setting up the treatments and preserved at 4 °C, were placed in the LOM layer to allow them to choose their "preferred" sediment. The total weight of earthworms was checked to be similar after gut defection for all EW treatments. Combined treatments were prepared, containing both plants and earthworms (P + EW). Treatments without any soil engineer represented the control (NT).

All mesocosms were incubated over a period of 8 weeks under controlled conditions in a climate chamber at 18 ± 3 °C, 65% humidity, 16/8 hour day-night time rhythm (Schomburg et al., 2018a). Soil moisture content was controlled twice a week over the total weight of the mesocosms. In case of a soil moisture deficit, mesocosms were rewetted using a fog irrigation nozzle in order to preserve aggregates created at the soil surface.

2.3. X-ray computed tomography (X-ray CT)

2.3.1. Mesocosm scanning

After eight weeks of incubation, mesocosms were prepared for X-ray CT analysis. Plant stems were cut off at the edge and mesocosms closed at both ends. The remaining space between the closure cap and the sediment was filled up with styrofoam chips, in order to prevent movement of the sediment layers during the scanning process. Mesocosms were scanned using a LightSpeed VCT (GE Medicalm Systems) medical scanner. The device was equipped with a rotating scanner emitting X-ray beams on a 1.2 mm focal spot with a peak energy of 120 keV and a tube current of 500 mA. Data acquisition was based on a 64 channel detector and an axial pitch of 0.625 mm. These settings were already predefined for the analysis of soil and peat samples in recent studies (Turberg et al., 2014; Amossé et al., 2015; Liernur et al., 2017; Schomburg et al., 2019). Each image of the sequence was projected on a 512 × 512 pixel grid and adapted to the transaxial field of view, defining a cubic voxel size of 0.3 × 0.3 × 0.3 mm on all 2D reconstructed CT images. On average, 1200 CT images were generated per mesocosm.

2.3.2. Image analysis

Raw images were treated using imageJ (open source software) (Schneider et al., 2012) and Avizo, version 9.3.0 (FEI, 2016). Raw images of each mesocosm were imported in imageJ and converted into one image sequence. Substacks were created individually for each image sequence and contact zones between the sediments and the PVC tubes were cut out. Image sequences were subsequently implemented in Avizo. Binarisation was performed in order to separate the mineral and organic matrix from the void representing plant root galleries, earthworm burrows, pores and cracks. Interactive thresholding was used, as the provided algorithms for automatic thresholdings did not accurately represent the features of interest (i.e. voids related to macro-biological engineering activity). Automatic thresholding using factorisation tended to overestimate root galleries in some image sequences, but did not vary significantly from interactive thresholding levels when considering all image sequences (Appendix 1c, d). In a first step, a specific threshold value was defined for each image sequence. The arithmetic mean of all individual threshold values applied on each image sequence was then calculated and set to 31,778. Binarisation was performed again on each image sequence using the arithmetic mean of the threshold levels. Since all scans were conducted with exactly the same measuring configuration, mean values did not lead to a significant over- or under-estimation of the voids (Appendix 1c). Porosity was calculated on the ratio of the thresholded void and the remaining soil material. Skeletonisation of the voids was subsequently performed on the binarised 3D images using the auto-skeleton function with a smoothing coefficient of 0.5 and 10 iterations (Fig. 2). The total number of segments and nodes and the total segment length, calculated through skeletonisation, were used as an indicator for macro-biological structuring activity in each material. All indicators were normalised per dm^3 due to a slight variation in the total volume of each material.

2.4. Sampling of aggregates and soil engineers

Mesocosms were opened after CT scanning. Plant roots were sampled by hand, carefully washed with tap water, oven-dried for 48 h and weighed. Earthworms were collected and weighed after gut defection. Macro-aggregates of 250–2000 µm in size (Tisdall and Oades, 1982) were sampled by hand individually in each layer by sieving over

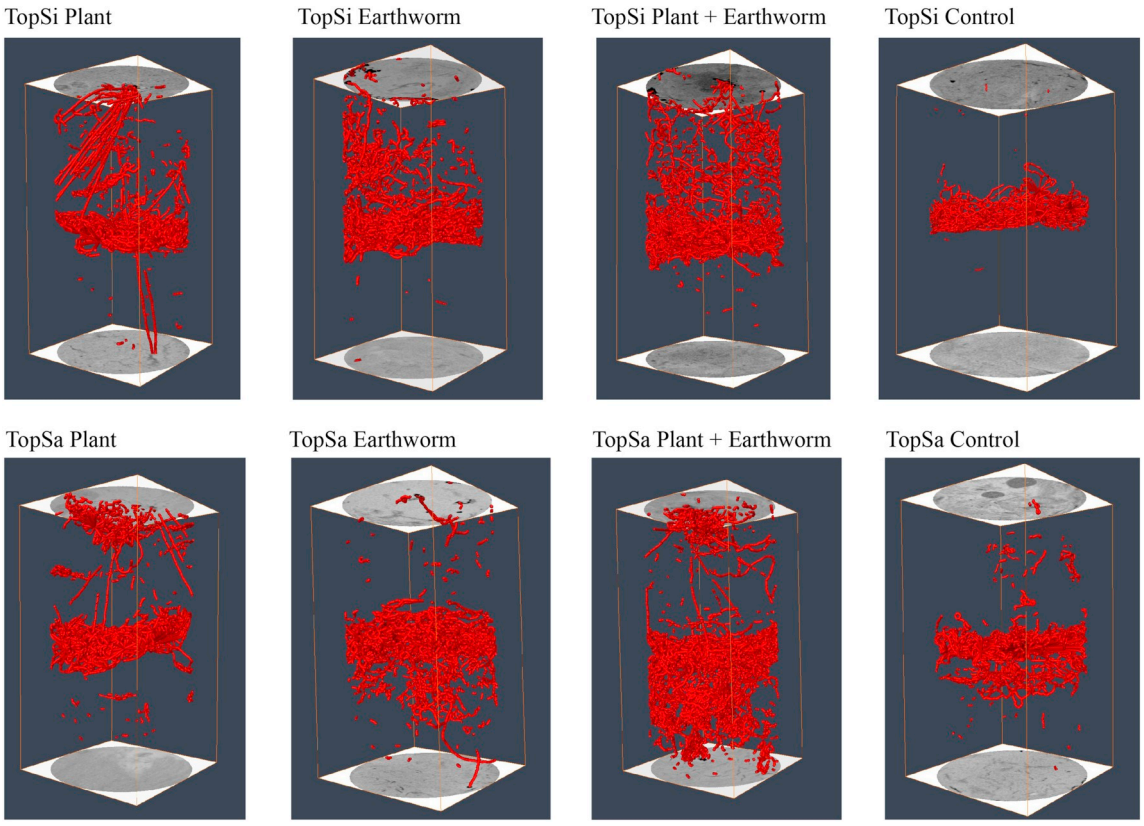

Fig. 2. Visualisation of 3D binarised elements for all treatments in both configurations performed in Avizo. Binarised items are illustrated by the red lines representing root galleries, earthworm burrows, pores and cracks. TopSi stays for the succession silt - buried litter - sand, TopSa for the succession sand – buried litter - silt. (For interpretation of the references to colour in this figure legend, the reader is referred to the web version of this article.)

2000 µm and then 250 µm (Schomburg et al., 2018a). Aggregate stability was determined over the proportion of water stable macro-aggregates (%WSA) in relation to the total amount of macro-aggregates collected from each layer. %WSA was determined according to the method described in Kemper and Rosenau (1986), using a modified automatic sieve-diving apparatus (Murer et al., 1993). Water-stable macro-aggregates and material from the control treatments were air-dried over an entire week and finely crushed for Rock-Eval pyrolysis.

2.5. Rock-Eval pyrolysis

OM dynamics during its incorporation into soil aggregates and its thermal stability were assessed using a Rock-Eval 6 pyrolyser (Vinci Technologies), which is described in Lafargue et al. (1998) and Behar et al. (2001). About 50–60 mg of finely crushed material from water-stable macro-aggregates was stepwise pyrolysed in an inert atmosphere and subsequently combusted using an artificial air supply. Released hydrocarbons were monitored by a flame ionisation detector (FID) and graphed as the "S2 thermogram", representing the sum of all released hydrocarbons. The analysis of the S2 thermogram provided information on OM bulk chemistry and thermal stability in soils and sediments (Disnar et al., 2003; Hetényi et al., 2005; Sebag et al., 2006). In this study, the area under the S2 curve was subdivided into to five areas (A1 to A5) with predefined temperature ranges: 200–340 °C for A1 (labile biopolymers), 340–400 °C for A2 (resistant biopolymers), 400–460 °C for A3 (immature geopolymers), and A4 and A5, which stands for refractory geopolymers (> 460 °C). These areas were used for the calculation of the R-index and I-index (Sebag et al., 2016). I-index was related to the thermally more labile fraction of OM and measures its degree of preservation as follows:

$$I - index = \log_{10}\left(\frac{A1 + A2}{A3}\right) \quad (1)$$

R-index was related to the whole OM content and measured the contribution of thermally more stable fractions as follows:

$$R - index = \frac{A3 + A4 + A5}{100} \quad (2)$$

The Rock-Eval I- and R-indices are independent from $CaCO_3$ and total organic carbon (TOC) contents. Moreover, the R-Index plotted against I-index is an indicator for the OM stability in aggregates. This diagram is a useful tool to describe complex processes by taking into account only two synthetic parameters: it graphically represents the complex transformations of soil organic constituents, even if their chemical composition is not precisely known (Sebag et al., 2016). These authors calibrated > 1000 soil samples from different soil horizons and indicated a strong correlation between I-index and R-index in non-disturbed soils, where changes in labile OM fraction drive the bulk thermal stability. Thus, the I/R diagram was shown to be pertinent to interpret the presence of OM in soil aggregates, especially in biogenic structures formed by soil engineering organisms (Schomburg et al., 2018a). The R-index representing OM thermal stability has been shown to be an especially powerful indicator for the degree of OM stabilisation in the bulk soil and in soil aggregates (Matteodo et al., 2018; Schomburg et al., 2018a).

2.6. Statistical data processing

All statistical analyses and data visualisations were performed in R (R Core Team, 2013) version 3.5.1. The package "easyanova" was used (Arnhold, 2013) for the split-plot data. The packages "ggplot2"

(Wickham, 2009) and "gridExtra" (Auguie, 2016) were used for data visualisation.

2.6.1. One-way analysis of variance (ANOVA)

Data collected at the level of the mesocosm (biomass and weight change) were analysed with a one-way analysis of variance (ANOVA). Normal distribution and variance homogeneity of the data were previously verified using the Shapiro-Wilk test and the Bartlett test. If significant, multiple comparisons at the main factor levels were identified using Tukey's HSD post-hoc test.

2.6.2. Analyses of variance for randomised split-plot designs

The role of the composition of the deposit, its superimposition, and the presence of soil engineers on the structuration patterns, soil structural stability and OM dynamics (see hypothesis in the Introduction section) were analysed using three analyses of variance for randomised split-plot designs. Three robust indicators for the structuration patterns (total segment length from X-ray CT), the degree of structuration indicated by water stable macro-aggregates (Six et al., 2000), and the R-index representing OM thermal stability in soil aggregates (Schomburg et al., 2018a) were defined as response variables. Two predictor variables were defined for each analysis: the factor "treatment" with four levels (P, EW, P + EW, NT) and the factor "layer" with five levels (silt.top, silt.bottom, sand.top, sand.bottom, LOM). The factor "layer" thus contained information about both the composition of the deposit and the position within the mesocosm. This information could not be analysed using two different predictor variables due to missing statistical independency. ANOVAs were performed using the sum of squares type III. Criteria for normality and homoscedasticity were checked prior to the analyses using the Shapiro-Wilk test and the Bartlett test. As the total segment length and the R-index failed the criteria for normality, data were logarithmised. Subsequent multiple comparison tests at the main factor levels were performed using Tukey's HSD test. Hypotheses were tested at an $\alpha = 0.05$ significance level, accepting the risk at a p-value < 0.05.

3. Results

3.1. Soil engineers

All earthworms survived and gained on average at least 20% weight in the TopSi configuration (Table 2). In the TopSa configuration, earthworms tended to lose weight in the EW treatment while they

Table 2
Root biomass and earthworm weight gain (EW weight gain) after the incubation in the two configurations TopSi and TopSa (mean ± SE). Negative values correspond to weight loss of earthworms. P stays for plant, EW for earthworm, P + EW for plant + earthworm and NT for control. ΔPlant + Root biomass indicates differences in plant + root biomass within eight weeks of incubation. Letters a and b stand for differences between the treatments in EW weight gain, root biomass and ΔPlant + Root biomass representing results from Tukey's HSD tests for one-way ANOVA at an $\alpha = 0.05$ significance level, accepting the risk at a p-value < 0.001.

Treatment	EW weight gain (%)	Root biomass (g)	ΔPlant + Root biomass (g)
TopSi			
P		2.50 ± 2.10[a]	6.55 ± 3.50[a]
EW	32.28 ± 12.90[a]		
P + EW	24.40 ± 9.32[a]	0.83 ± 0.46[a]	4.83 ± 3.91[a]
NT			
TopSa			
P	1.69 ± 0.77[a]	16.89 ± 3.63[b]	
EW	−8.96 ± 8.20[a]		
P + EW	13.81 ± 14.05[a]	1.61 ± 0.89[a]	9.13 ± 5.12[a,b]
NT			

Table 3
Results for the analyses of variance for randomised split-plot designs. Significant overall and interaction effects were specified by a p-value < 0.05. "n.s." stays for not significant. Letters a, b, c and d represent results from Tukey's HSD posthoc analysis at an $\alpha = 0.05$ significance level accepting the risk at a p-value < 0.001. ":" represents interaction effects between two predictor variables.

Predictor variables and levels	Response variables		
	Total segment length	%WSA	R-index
Overall and interaction effects			
Treatment	$p < 0.001$	$p < 0.05$	n.s.
Layer	$p < 0.001$	$p < 0.001$	$p < 0.001$
Treatment: Layer	$p < 0.001$	$p < 0.05$	$p < 0.001$
Multiple comparisons of treatments			
Plant	b	ab	a
Earthworm	a	b	a
Plant + earthworm	a	a	a
Control	b	c	a
Multiple comparisons of layers			
silt.top	b	ab	c
silt.bottom	bc	ab	c
sand.top	bc	b	a
sand.bottom	c	c	a
LOM	a	a	b
Multiple comparisons of treatments within layer levels			
silt.top			
Plant	ab	a	ab
Earthworm	a	a	ab
Plant + earthworm	ab	a	a
Control	b	a	b
silt.bottom			
Plant	a	b	a
Earthworm	a	a	b
Plant + earthworm	a	a	a
Control	a	b	a
sand.top			
Plant	a	a	b
Earthworm	a	bc	a
Plant + earthworm	a	ab	b
Control	a	c	b
sand.bottom			
Plant	a	a	a
Earthworm	a	a	a
Plant + earthworm	a	a	a
Control	a	a	a
LOM			
Plant	b	a	a
Earthworm	a	a	b
Plant + earthworm	a	a	a
Control	b	a	a
Multiple comparisons of layers within treatment levels			
Plant (P)			
silt.top	b	ab	b
silt.bottom	b	b	ab
sand.top	b	a	a
sand.bottom	b	b	a
LOM	a	a	a
Earthworm (EW)			
silt.top	b	ab	c
silt.bottom	bc	a	d
sand.top	c	bc	a
sand.bottom	c	c	b
LOM	a	ab	cd
Plant + earthworm (P + EW)			
silt.top	b	b	b
silt.bottom	b	a	b
sand.top	b	ab	a
sand.bottom	b	b	a
LOM	a	b	b
Control (NT)			
silt.top	b	a	d
silt.bottom	b	ab	c
sand.top	b	b	ab
sand.bottom	b	b	a
LOM	a	a	bc

seemed to gain weight in the P + EW treatment, but the differences were not significant. Values for root biomass were similar in all treatments containing plants in both configurations except for P + EW treatment in the TopSi configuration, in which root biomass tended to be reduced. Plant biomass (shoots and roots) significantly increased in the P treatment in the TopSa configuration compared to the P and the P + EW treatment in the TopSi configuration (p-value < 0.001).

3.2. X-ray computed tomography (X-ray CT)

Macroporosity, total segment length, and the number of segments were strongly correlated ($r_{pearson}$ > 0.94). Therefore, total segment length was defined as a robust indicator to analyse the structuration patterns (see Section 2.6). The contribution of the predictors "treatment" and "layer" to explain the variability of the total segment length was highly significant (p-value < 0.001) (Table 3). Furthermore, interaction terms between "treatment" and "layer" were highly significant (p-value < 0.001) (Table 3), indicating that the effect of "treatment" varied within the five levels of "layer". Multiple comparisons at the main factor level within "treatment" indicated that the treatments EW and P + EW significantly increased the total segment length. Within the level of "layers", total segment length was greatest in LOM, followed by silt.top. Total segment length was lowest in the sand.bottom layer (Tables 3, 4). Regarding interaction terms, earthworms significantly increased the total segment length in the silt.top and in the LOM layer. Plants tended to increase the total segment length in the top layers only, but interaction terms were not significant (Tables 3, 4).

3.3. Aggregate stability

The percentage of water-stable macro-aggregates was significantly affected by both predictors tested. The overall effect of "layer" was highly significant (p-value < 0.001) and the effect of "treatment" was significant (p-value < 0.05). Interaction terms between "treatment" and "layer" were also significant (p-value < 0.05) (Table 3). Multiple comparisons at the main factor level within the four levels of "treatment" indicated that aggregate stability is generally highest in P + EW followed by P and EW (Tables 3, 4). Multiple comparisons at the main factor level within the five levels of "layer" highlighted the greatest aggregate stability in the LOM-layer followed by the silt layers regardless of its position, and the top.sand and the bottom.sand layer. Regarding interaction terms, the presence of earthworms significantly improved aggregate stability in the silt.bottom layer, whereas the presence of plants positively contributed to aggregate stability in the sand.top layer (Tables 3, 4).

Table 4
Mean values ± SE for robust indicators selected for soil structural stability, structuration patterns, and OM dynamics. Values are given for the four levels of "treatment" within the five levels of "layer". WSA: water stable macro-aggregates; P: plant, EW: earthworm, P + EW: plant + earthworm, NT: control.

Layer & treatment	Total segment length (mm dm^{-3})	WSA (%)	R-index	I-index
silt.top				
P	1979 ± 1412	10.68 ± 0.84	0.57 ± 0.01	0.20 ± 0.02
EW	5668 ± 1263	9.53 ± 2.17	0.58 ± 0.01	0.18 ± 0.01
P + EW	3416 ± 1000	9.87 ± 2.86	0.59 ± 0.01	0.18 ± 0.01
NT	114 ± 112	9.17 ± 0.95	0.56 ± 0.01	0.22 ± 0.01
silt.bottom				
P	90 ± 67	7.55 ± 2.05	0.60 ± 0.01	0.17 ± 0.01
EW	2878 ± 1126	12.50 ± 2.92	0.56 ± 0.01	0.22 ± 0.01
P + EW	2639 ± 1186	14.02 ± 2.99	0.59 ± 0.02	0.19 ± 0.01
NT	92 ± 73	7.99 ± 1.39	0.59 ± 0.01	0.17 ± 0.01
sand.top				
P	1017 ± 223	13.39 ± 4.58	0.62 ± 0.01	0.18 ± 0.02
EW	1013 ± 140	7.39 ± 2.03	0.68 ± 0.05	0.17 ± 0.03
P + EW	1515 ± 438	10.72 ± 3.10	0.63 ± 0.01	0.20 ± 0.01
NT	109 ± 50	4.67 ± 3.08	0.63 ± 0.01	0.24 ± 0.01
sand.bottom				
P	30 ± 16	6.07 ± 4.02	0.62 ± 0.03	0.21 ± 0.03
EW	193 ± 53	4.35 ± 2.43	0.63 ± 0.03	0.15 ± 0.02
P + EW	167 ± 41	7.65 ± 1.94	0.63 ± 0.01	0.18 ± 0.01
NT	24 ± 18	4.77 ± 1.42	0.63 ± 0.01	0.20 ± 0.01
LOM				
P	29,966 ± 7269	13.87 ± 4.13	0.61 ± 0.02	0.18 ± 0.02
EW	34,651 ± 8008	11.72 ± 2.94	0.57 ± 0.01	0.21 ± 0.02
P + EW	34,401 ± 3806	10.83 ± 1.21	0.59 ± 0.02	0.17 ± 0.02
NT	23,140 ± 4083	10.31 ± 2.23	0.61 ± 0.03	0.16 ± 0.03

3.4. Rock-Eval pyrolysis

R-index values ranged between 0.55 and 0.67 and I-index values between 0.12 and 0.25. R- and I-indices were strongly correlated in silty sediment ($r_{pearson}$ = 0.97 and 0.72) and less in the LOM layer in both configurations ($r_{pearson}$ = 0.67). No clear correlation was found in the respective sand layers (Fig. 3). OM thermal stability represented by the R-index was significantly affected by "layer" (p-value < 0.001) (Table 3). "Treatment" did not have any significant effect on OM thermal stability. Interactions terms between "treatment" and "layer" were highly significant (p-value < 0.001) (Table 3). Within the five levels of "layer", R-index values were greatest in the sand layers, followed by the LOM and the silt layers (Tables 3, 4). Regarding interaction terms, the effect of EW varied strongly within the five levels of "layer": EW significantly increased the R-index in the sand.top layer and decreased the R-index in the silt.bottom and the LOM layers (Table 4, Fig. 3). Plants alone (P) and earthworms (EW) significantly decreased the R-index in the silt.top layer compared to P + EW. R-index values for P + EW treatments tended to range between values for P and EW in the sand.top, sand.bottom and the LOM layer (Fig. 3).

4. Discussion

4.1. Behaviour of ecosystem engineers

As assumed in the main hypothesis, the treatment, the composition and superimposition of the layers strongly affected the structuration patterns in the mesocosms. Plant and earthworms' bioturbation activities are thus strongly controlled by the physico-chemical properties of the deposits.

Roots of the pioneer plant *P. arundinacea* spread out only in the top layers, although they could reach the bottom of the mesocosm within a similar timeframe as observed in a preliminary experiment (data not shown). Regardless of the configuration, roots did not enter the underlaying LOM layer suggesting that this layer was either unfavourable for rooting, or that sufficient amounts of nutrients and water were available above. The root biomass was smaller in silty sediments compared to sandy ones. As sand retains less water and nutrients, plants had to extend their roots to reach water and nutrient sources, probably provided at the top of LOM layers. Contrary to our expectations, a fine sediment texture and buried litter might delay the structuration progression whereas coarse sandy deposits favour a fast colonisation by roots. The water availability could probably also be decisive but was not investigated in the present study.

The earthworms *A. chlorotica* were found either in the silt or in the LOM layer, independent of the configuration. This highlights their preference for food resource and finer soil textures (Table 1) (Edwards and Bohlen, 1996). Lavelle et al. (1997) underlined that endogeics prefer to move into topsoil layers that may explain why *A. chlorotica* dug in sand in TopSa configuration. Moreover, this worm is a pioneer species commonly abundant in disturbed soils, for instance in the very pioneer area in floodplains composed of bare soils with gravels

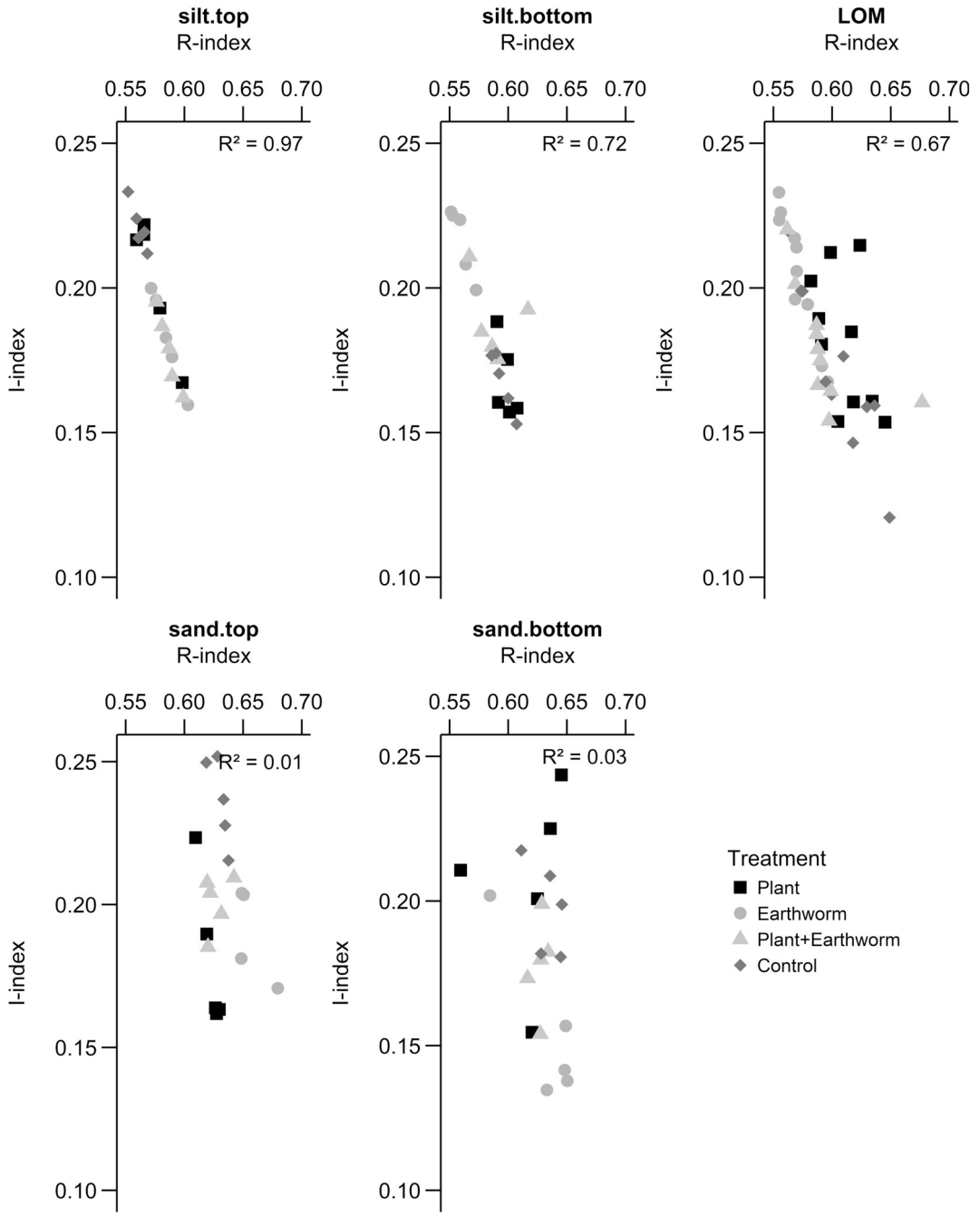

Fig. 3. R-index plotted against I-index as an indicator for OM thermal stabilisation in aggregates.

colonised by herbaceous vegetation (Fournier et al., 2012; Amossé et al., 2015). Bouché (1972) also mentioned that *A. chlorotica* is found in urban human-perturbed environment (e.g. building sites) that are returning to their equilibrium states. Amossé et al. (2015) and Vergnes et al. (2017) also observed this species in Anthrosols and Technosols.

Focusing on the combination treatment P + EW, total segment length was surprisingly not increased compared to P and/or EW alone. Our main hypothesis is that mutual beneficial effects might not have been possible to be visualised with X-ray CT, as each soil engineer could have taken advantage of their respective structures. Plants are known to use earthworm burrows for rooting, as burrow-linings are enriched in available nutrients and provide easier pathways for root network extension. Burrow walls but also casts are furthermore hotspots of nutrients, making them preferentially colonised by plant roots (Spiers et al., 1986; Zaller and Arnone, 1999; Decaëns et al., 2011). However, in our study, the distinction of root galleries and earthworm burrows was not possible with the resolution of the X-ray CT. Further research is still needed regarding this topic by using higher resolution technics.

4.2. Aggregate stability

The percentage of water-stable macro-aggregates varied significantly among the treatments and within the layers. Aggregate stability is generally thought to be positively correlated to the proportion of silt and clay and negatively correlated to the proportion of sand (Lavelle et al., 1997; Duiker et al., 2003; Kaiser et al., 2012).

In our study, the highest aggregate stability was found in the LOM layer. OM components are efficient bonding agents that agglutinate soil particles (Tisdall and Oades, 1982; Guggenberger et al., 1996; Kong et al., 2005; Jouquet et al., 2008). Moreover, they stimulate fungal and

bacterial activities as well as an active root growth, all of them being biological aggregate formation agents (Six et al., 2002). In the P treatment, OM can thus favour the presence of bacteria and fungi in the vicinity of plant roots, thus enhancing the formation of aggregates inside LOM layer. In the presence of earthworms, these effects are probably enhanced due to the mucus released by *A. chlorotica* when passing through the LOM layer.

Focusing on sediment layers, *A. chlorotica* did not increase aggregate stability, except for the silt.bottom layer. Earthworms usually increase aggregation processes (Fonte and Six, 2010), but sometimes not (Fonte et al., 2012; Lubbers et al., 2017). Indeed, *A. chlorotica* is known to decrease aggregate stability (Milleret et al., 2009b) and our result confirm the importance of taking into account the community composition of earthworms instead of one single species. The location of organic matter (onto the soil surface or directly mixed in the soil matrix) is also an important feature regarding soil bioturbation, especially for endogeic species (Le Couteulx et al., 2015). The presence of an LOM layer may have disturbed the ecological behaviour of *A. chlorotica*.

Combining earthworms and plants slightly increased aggregate stability, which was mainly due to the fact that plants and earthworms were almost never present in the same sediment, except for the silt.top layer. However, the contribution of *P. arundinacea* was the highest on aggregation, especially in the sand.top layer. Plant roots were thus the most efficient binding agents as also reported by Fonte et al. (2012) and Kohler-Milleret et al. (2013).

4.3. OM dynamics

4.3.1. Mechanisms of OM incorporation into soil aggregates

In near-natural soils, the strong correlation between R- and I-indices has two main origins: on the one hand, mineralisation of OM leads to a decrease in I-index values and simultaneously to an increase of R-index values (Albrecht et al., 2015). On the other hand, strong interactions between OM and mineral matter results in a specific range shift of R-index and I-index values (Sebag et al., 2016), especially in soil aggregates, as already reported by Schomburg et al. (2018a).

In our study, except in the TopSa configuration where root exudates favoured bindings, R-index and I-index were not correlated in sandy textures, possibly because the low specific surface of fine sand particles minimize OM-sandy grains' interaction. On the contrary, R-index and I-index were correlated in the silt and LOM layer. This reinforces our findings on aggregate stability and thus highlighting the involvement of soil engineers. Root exudates promote OM mineralisation by stimulating microbial activities and *A. chlorotica*, mostly found in the silt and LOM layers, enhanced the mixing both materials into biogenic aggregates.

4.3.2. OM thermal stability

Contrary to our expectations, OM thermal stability was increased in sandy sediments, while it is usually the highest in the presence of fine sediment textures such clay and silt (Sollins et al., 1996; Bronik and Lal, 2005).

In our experiment, the OM thermal stability in aggregates formed by roots was low mainly due to exudates that contain easy decomposable OM. Such labile OM generally underlies fast microbial decay, unless OM is physically protected by mineral particles (Sollins et al., 1996). The fine mineral fraction can occlude labile OM, enabling its efficient protection against microbial decay, which can improve the persistence of labile OM in the soil (Schmidt et al., 2011). In our case, the silty texture was not fine enough to assume this role.

In the presence of earthworms, R-index values were generally constant in the sand layers, but increased in the silt and the LOM layers, regardless of the configuration. Thus, earthworms increased the thermal stability of OM in the silt. In the sand, earthworms only associated mineral and organic particles without improving its thermal stability. We, therefore, assume that earthworm movements only displaced OM without passing through their digestive tract. Earthworms generally avoid digesting the sandy soil fraction as it causes intestinal damages in their gut system (Curry and Schmidt, 2007). Nevertheless, earthworm movements seem powerful enough to mix sand particles with OM from the underlying LOM layers. This hypothesis is supported by the R-index value which was similar in the sand and the LOM layer in the TopSa configuration. On the other hand, earthworms generally promote OM sequestration into soil aggregates, especially in finer soil textures (Lavelle, 1988; Frouz et al., 2015; Angst et al., 2017). In the silt, earthworms excreted easier decomposable OM, such as mucus and saliva, which agglutinated soil particles during the gut transit. Simultaneously, earthworms incorporated more recalcitrant compounds from the bulk soil, such as lignin, into their casts (Lavelle et al., 1997), corresponding to thermally resistant OM (Disnar et al., 2003).

In most of the layers, in which plants and earthworms were concomitantly present, R-index values for P + EW treatments ranged between values for P and EW. Similar observations for the thermal stability of OM were reported by Schomburg et al. (2018a) in a mesocosm experiment. However, these authors could not distinguish whether these values resulted from (1) an interaction between plants and earthworms during OM transformation into aggregates as proposed by Zangerlé et al. (2014) or (2) if they resulted from a positive feedback between both engineers, individually modifying the thermal stability of OM. However, recent studies reported that plants inhabited earthworm casts to take advantage of the enriched amount of nutrients (Spiers et al., 1986; Zaller and Arnone, 1999; Decaëns et al., 2011). Conversely, earthworms prefer feeding on root-derived carbon and easy decayable OM from fine roots and incorporate this carbon into soil aggregates (Gilbert et al., 2014; Sanchez-de Leon et al., 2014; Yavitt et al., 2015).

4.4. Limitations of the mesocosm approach

Combining X-ray CT and Rock-Eval pyrolysis was suitable for analysing structuration patterns of soil engineers and OM thermal stability in soil aggregates in an artificially constructed floodplain soil. The experimental design was an innovative approach and provided highly useful data, but several aspects need to be addressed in greater detail. Hence, results obtained for the P + EW treatment were difficult to interpret. Using Rock-Eval pyrolysis, a mixed signature was found, which either represented interaction or an additive effect of engineer specific indices. Plant root galleries and earthworm burrows could not be differentiated using X-ray CT, at least not with the intermediate resolution provided by the medical scanner. Increasing the resolution of the X-ray CT scanner constitutes a significant challenge because it requires a smaller diameter of the samples and is very expensive. In the present study, downscaling the size of the mesocosm was not compatible with earthworm requirements in terms of living space and would have led to a loss of information about the structuration patterns. Alternatively, subsampling might have impacted aggregate sampling and collection of ecosystem engineers. Nevertheless, the use of high resolution X-ray CT is probably one of the key approaches for an increased understanding of plant-earthworm interactions. Furthermore, several studies indicate that aggregate stability cannot be significantly improved in short-term mesocosm experiments (Bossuyt et al., 2005; Milleret et al., 2009a). Extending the incubation period might, however, result in clearer data, e.g. increased stability of aggregates formed by earthworms, or more distinctive OM signatures which can be easier identified by Rock-Eval pyrolysis.

5. Conclusions

Soil structuration and mechanisms of OM stabilisation in plants and earthworms' soil aggregates were identified through a mesocosm design using a superimposition of different materials layers, similar to what occurs during flood events in a near-natural floodplain. We employed a

novel combination of X-ray CT and Rock-Eval pyrolysis in our analysis. We showed that structuration patterns and aggregate stability depend on the soil engineer and the composition as well as the superimposition of the layers. Buried litter layers provide OM inputs that promote initial soil aggregate formation. However, if the overtopping layer supplies a sufficient nutrient stock for soil engineering organisms, buried litter delays this process. Thus, the structural stability can vary significantly with depth in an alluvial soil. Moreover, OM dynamics and thermal stabilisation result from a complex interplay between soil engineers and the initial composition of deposits, and could not be attributed to general effects of one specific soil engineer. Our results suggest that the superimposition of layers (sand on top of an organic layer followed by silt) might be the best configuration of a floodplain soil to develop. This soil structure formation is favoured by plants and is most the most efficient to promote OM sequestration by earthworms in the subsoil.

Acknowledgements

This work was developed as a part of the FloodSTRESS project funded by the Swiss National Science Foundation (SNF), project no. FN 315230_153460, and CCES-project RECORD Catchment of the ETH domain. The authors gratefully thank the University Center for Legal Medicine Lausanne – Geneva (CURML), especially Kewin Ducrot for X-ray CT analysis and the FiBL institute in Frick, especially Anton Kuhn and Simon Tresch for providing equipment for mechanical sediment sieving and for aggregate stability analysis. They furthermore thank the following people for their great support during field and lab work: Guillaume Fayet for sediment sampling, Bernhard Stehle for soil sieving, Manon Moschard and Marie Duval for mesocosm construction, Théodore Hafen for humidity control during the incubation experiment, Florian Migliarini for transport services, Franziska Fischer for sediment analyses and Rock-Eval sample preparation, and Karin Verrecchia for her careful editing of the first version of the manuscript.

Appendix A

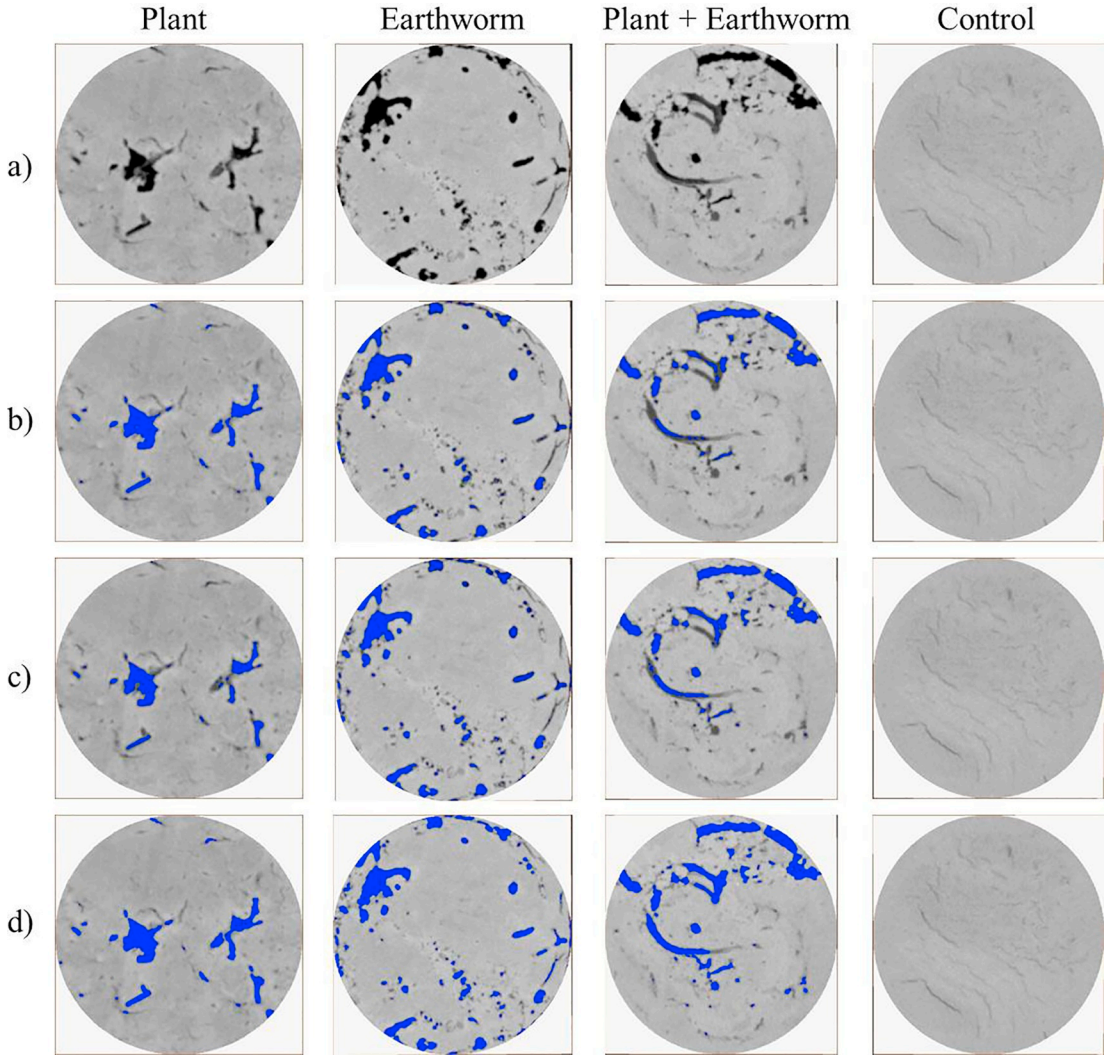

Appendix 1. Comparison between different binarisation methods for the treatments performed in Avizo. Thresholded voids are coloured in blue. a) shows the raw image, b) the individual threshold value specifically selected for this image, c) the arithmetic mean of all threshold values for each image set, and d) the automatic thresholding using factorisation.

References

Acreman, M.C., Riddington, R., Booker, D.J., 2003. Hydrological impacts of floodplain restoration: a case study of the River Cherwell, UK. Hydrol. Earth Syst. Sci. 7, 75–85.

Albrecht, R., Sebag, D., Verrecchia, E., 2015. Organic matter decomposition: bridging the gap between Rock-Eval pyrolysis and chemical characterization (CPMAS C-13 NMR). Biogeochemistry 122, 101–111.

Amossé, J., Turberg, P., Kohler-Milleret, R., Gobat, J.-M., Le Bayon, R.-C., 2015. Effects of endogeic earthworms on the soil organic matter dynamics and the soil structure in urban and alluvial soil materials. Geoderma 243–244, 50–57.

Angers, D.A., Caron, J., 1998. Plant-induced changes in soil structure: processes and feedbacks. Biogeochemistry 42, 55–72.

Angst, Š., Mueller, C.W., Cajthaml, T., Angst, G., Lhotáková, Z., Bartuška, M., Špaldaňova, A., Frouz, J., 2017. Stabilisation of soil organic matter by earthworms is connected with physical protection rather than with chemical changes of organic matter. Geoderma 289, 29–35.

Arnhold, E., 2013. Package in the R environment for analysis of variance and complementary analyses. Braz. J. Vet. Res. Anim. Sci. 50 (6), 488–492.

Auguie, B., 2016. gridExtra: miscellaneous functions for "grid" graphics. https://CRAN.R-project.org/package=gridExtra.

Behar, F., Beaumont, V., Penteado, de B., Penteado, H. L., 2001. Rock-Eval 6 technology: performances and developments. *Oil Gas Sci. Technol.* 56: 111–134.

Blanchart, E., Lavelle, P., Braudeau, E., Le Bissonais, Y., Valentin, C., 1997. Regulation of soil structure by geophagous earthworm activites in humid savannas of Côte d'Ivoire. Soil Biol. Biochem. 29, 431–439.

Blouin, M., Hodson, M.E., Delgado, E.A., Baker, G., Brussaard, L., Butt, K.,.R., Dai, J., Dendooven, L., Peres, G., Tondoh, J.E., Cluzeau, D., Brun, J.-J., 2013. A review of earthworm impact on soil function and ecosystem services. Eur. J. Soil Sci. 64, 161–182.

Bossuyt, H., Six, J., Hendrix, P.F., 2005. Protection of soil carbon by microaggregates within earthworm casts. Soil Biol. Biochem. 37, 251–258.

Bouché, M., 1972. Lombriciens de France. Ecologie et systématique INRA Publ. Institut National des Recherches Agriculturelles, Paris.

Bronik, C.J., Lal, R., 2005. Soil structure and management: a review. Geoderma 124, 3–22.

Brown, G.G., Barois, I., Lavelle, P., 2000. Regulation of soil organic matter dynamics and microbial activity in the drilosphere and the role of interactions with other edaphic functional domains. Eur. J. Soil Biol. 36, 177–198.

Bullinger-Weber, G., Le Bayon, R.-C., Guenat, C., Gobat, J.-M., 2007. Influence of some physicochemical and biological parameters in soil structure formation in alluvial soils. Eur. J. Soil Biol. 43, 57–70.

Bullinger-Weber, G., Guenat, C., Gobat, J.-M., Le Bayon, R.-C., 2012. Impact of flood deposits on earthworm communities in alder forests from a subalpine floodplain (Kandersteg, Switzerland). Eur. J. Soil Biol. 49, 5–11.

Capowiez, I., Sammartino, S., Michel, E., 2011. Using X-ray tomography to quantify earthworm bioturbation non-destructively in repacked soil cores. Geoderma 162, 124–131.

Capowiez, I., Bottinelli, N., Sammartino, S., Jouquet, P., 2015. Morphological and functional characterisation of the burrow systems of six earthworm species (Lumbricidae). Biol. Fertil. Soils 51, 869–877.

Coppola, E., Capra, G., Odierna, P., Vacca, S., Buondonno, A., 2010. Lead distribution as related to pedological features of soils in the Volturno river low basin (Campania, Italy). Geoderma 159, 342–349.

Curry, J.P., Schmidt, O., 2007. The feeding ecology of earthworms: a review. Pedobiologia 50, 463–477.

Czarnes, S., Hallett, P.D., Bengough, A.G., Young, I.M., 2000. Root- and microbial- derived mucilages affect soil structure and water transport. Eur. J. Soil Sci. 51, 435–443.

De Vivo, B., Sommer, R., Ayuso, R., Calderoni, G., Lima, A., Pagliuca, S., Sava, A., 2001. Pb isotopes and toxic metals in floodplain and stream sediments from the volturno river basin, Italy. Environ. Geol. 41, 101–112.

Decaëns, T., Margerie, P., Renault, J., Bureau, F., Aubert, M., Hedde, M., 2011. Niche overlap and species assemblace dynamics in an aging pasture gradient in north-western France. Acta Oecologica-Intern.. J. Ecol. 37, 212–219.

Degens, B.P., Sparling, G.P., Abbott, L.K., 1994. The contribution from hyphae, roots and organic carbon constituents to the aggregation of a sandy loam under long-term clover-based and grass pastures. Eur. J. Soil Sci. 45, 459–468.

Diaz-Zorita, M., Perfect, E., Grove, J., 2002. Disruptive methods for assessing soil structure. Soil Tillage Res. 64, 3–22.

Disnar, J.R., Guillet, B., Keravis, D., Di-Giovanni, C., Sebag, D., 2003. Soil organic matter (SOM) characterization by Rock-Eval pyrolysis: scope and limitations. Org. Geochem. 34, 327–343.

Duiker, S.W., Rhoton, F.E., Torrent, J., Smeck, N.E., Lal, R., 2003. Iron (hydr)oxide crystallinity effects on soil aggregation. Soil Sci. Soc. Am. J. 67, 606–611.

Edwards, C.A., Bohlen, P.J., 1996. Biology and Ecology of Earthworms, Band 3. Springer Science & Business Media.

FEI, 2016. Amira & Avizo 3D software. URL. https://www.fei.com/software/amira-avizo/, Accessed date: 1 March 2017.

Fonte, S.J., Six, J., 2010. Earthworms and litter management contributions to ecosystem services in a tropical agroforestry system. Ecol. Appl. 20, 1061–1073.

Fonte, S.J., Quintero, D.C., Velasquez, E., Lavelle, P., 2012. Interactive effects of plants and earthworms on the physical stabilization of soil organic matter in aggregates. Plant Soil 359, 205–214.

Fournier, B., Samaritani, E., Shrestha, E., Mitchell, E.A.D., Le Bayon, R.-C., 2012. Community ecology of earthworm in a restored floodplain and potential as bioindicators of river restoration. Appl. Soil Ecol. 59, 87–95.

Frouz, J., Špaldoňová, A., Lhotáková, Z., Cajthaml, T., 2015. Major mechanisms contributing to the macrofauna-mediated slow down of litter decomposition. Soil Biol. Biochem. 91, 23–31.

Gilbert, K.J., Fahey, T.J., Maerz, J.C., Sherman, R.E., Bohlen, P., Dombroskie, J.J., Groffman, P.M., Yavitt, J.B., 2014. Exploring carbon flow through the root channel in a temperate forest soil food web. Soil Biol. Biochem. 76, 45–52.

Guenat, C., Bureau, F., Weber, G., Toutain, F., 1999. Initial stages of soil formation in a riparian zone: importance of biological agents and lithogenic inheritance in the development of the soil structure. Eur. J. Soil Biol. 35, 153–161.

Guggenberger, G., Thomas, R.J., Zech, W., 1996. Soil organic matter within earthworm casts of an anecic-endogeic tropical pasture community, Colombia. Appl. Soil Ecol. 3, 263–274.

Gurnell, A., Petts, G., 2002. Island-dominated landscapes of large floodplain rivers, a European perspective. Freshw. Biol. 47, 581–600.

Gurnell, A., Petts, G., 2006. Trees as riparian engineers: the Tagliamento River, Italy. Earth Surf. Process. Landf. 31, 1558–1575.

Helliwell, J.R., Sturrock, C.J., Grayling, K.M., Tracy, S.R., Flavel, R.J., Young, I.M., Whalley, W.R., Mooney, S.J., 2013. Applications of X-ray computed tomography for examining biophysical interactions and structural development in soil systems: a review. Eur. J. Soil Sci. 64, 279–297.

Heténi, M., Nyilas, T., Tóth, T.M., 2005. Stepwise Rock-Eval pyrolysis as a tool for typing heterogeneous organic matter in soils. J. Anal. Appl. Pyrolysis 74, 45–54.

IUSS Working Group WRB, 2015. World Reference Base for Soil Resources 2014, update 2015. International soil classification system for naming soils and creating legends for soil maps. World Soil Resources Reports No. 106. FAO, Rome.

Jouquet, P., Bottinelli, N., Podwojewski, P., Hallaire, V., Duc, T.T., 2008. Chemical and physical properties of earthworm casts as compared to bulk soil under a range of different land-use systems in Vietnam. Geoderma 146, 231–238.

Kaiser, M., Ellerbrock, R.H., Wulf, M., Dultz, S., Hierath, C., Sommer, M., 2012. The influence of mineral characteristics on organic matter content, composition, and stability of topsoils under long-term arable and forest land use. J.Geophys. Res.-Biog. 117, 1–16.

Kemper, W.D., Rosenau, R.C., 1986. Aggregate stability and size distribution. In: K. e. American Society of Agronomy - Soil Science Society of America (Ed.), Methods of Soil Analysis, Part 1. Agronomy Monograph no 9. ASA and SSSA, Madison, WI, pp. 425–442.

Kercheva, M., Sokołowska, Z., Hajnos, M., Skic, K., Shishkov, T., 2017. Physical parameters of Fluvisols on flooded and non-flooded terraces. Intern. Agro. 31, 73–82.

Kohler-Milleret, R., Le Bayon, R.-C., Chenu, C., Gobat, J.-M., Boivin, P., 2013. Impact of two root systems, earthworms and mycorrhizae ont the physical properties of an unstable silt loam Luvisol and plant production. Plant Soil 370, 251–265.

Kong, A.Y.Y., Six, J., 2010. Tracing roots vs. residue carbon into soils from conventional and alternative cropping systems. Soil Sci. Soc. Am. J. 74, 1201–1210.

Kong, A.Y.Y., Six, J., Bryant, D.C., Denison, R.F., van Kessel, C., 2005. The relationship between carbon input, aggregation, and soil organic carbon stabilization in sustainable cropping systems. Soil Sci. Soc. Am. J. 69, 1078–1085.

Lafargue, E., Marquis, F., Pillot, D., 1998. Rock-Eval 6 applications in hydrocarbon exploration, production, and soil contamination studies. Rev.l'Inst. Fran. Pét. 53, 421–437.

Lavelle, P., 1988. Earthworm activites and the soil system. Biol. Fertil. Soils 6, 237–251.

Lavelle, P., Spain, A., 2001. Soil Ecology. Springer, Netherlands. https://doi.org/10.1007/0-306-48162-6.

Lavelle, P., Bignell, D., Lepage, M., Wolters, V., Roger, P., Ineson, P., Heal, O.W., Dhillion, S., 1997. Soil function in a changing world: the role of invertebrate ecosystem engineers. Eur. J. Soil Biol. 33, 159–193.

Le Bayon, R.-C., Bullinger-Weber, G., Gobat, J.-M., Guenat, C., 2013. Chapter 3: earthworm communities as indicators for evaluating floodplain restoration success in floodplains, environmental management, restoration and ecological implications. In: Environemental Research Advances. Enner Herenio Alcantara. Nova publishers, New York (241 pp.).

Le Bayon, R.C., Bullinger-Weber, G., Schomburg, A., Turberg, P., Schlaepfer, R., Guenat, C., 2017. Earthworms as ecosystem engineers: a review. In: Earthworms: Types, Roles and Research. NOVA Science Publishers, New York, pp. 129–178.

Le Couteulx, A., Wolf, C., Hallaire, V., Pérès, G., 2015. Burrowing and casting activities of three endogeic earthworm speices affected by organic matter location. Pedobiologia 58, 97–103.

Liernur, A., Schomburg, A., Turberg, P., Guenat, C., Le Bayon, R.-C., Brunner, P., 2017. Coupling X-ray computed tomography and freeze-coring for the analysis of fine-grained low-cohesive soils. Geoderma 308, 171–186.

Lin, H., Bouma, J., Wilding, L.P., Richardson, J.L., Kutílek, M., Nielsen, D.R., 2005. Advances in hydropedology. Adv. Agron. 85, 1–89.

Lubbers, I.M., Pulleman, M.M., Van Groenigen, J.W., 2017. Can earthworms simultaneously enhance decomposition and stabilization of plant residue carbon? Soil Biol. Biochem. 105, 12–24.

Malmqvist, B., Rundle, S., 2002. Threats to the running water ecosystems of the world. Environ. Conserv. 29, 134–153.

Marriot, S.B., 1998. Channel-Floodplain Interactions and Sediment Deposition on Floodplains.

Matteodo, M., Grand, S., Sebag, D., Rowley, M.C., Vittoz, P., Verrecchia, E.P., 2018. Decoupling of topsoil and subsoil controls on organic matter dynamics in the Swiss Alps. Geoderma 330, 41–51.

Milleret, R., Le Bayon, R.-C., Gobat, J.M., 2009a. Root, mycorrhiza and earthworm interactions: their effects on soil structuring processes, plant and soil nutrient concentration and plant biomass. Plant Soil 316, 1–12.

Milleret, R., Le Bayon, R.-C., Lamy, F., Gobat, J.M., Boivin, P., 2009b. Impact of roots,

mycorrhizas and earthworms on soil physical properties as assessed by shrinkage analysis. J. Hydrol. 373, 499–507.
Murer, E.J., Baumgarten, A., Eder, G., Gerzabek, M.H., Kandeler, E., Rampazzo, N., 1993. An improved sieving machine for estimation of soil aggregate stability (SAS). Geoderma 56, 539–547.
Nanson, G.C., Croke, J.C., 1992. A generic classification of floodplains. Geomorphology 4, 459–486.
Pierret, A., Capowiez, I., Moran, C.J., Kretzschmar, A., 1999. X-ray Computed Tomography to quantify tree rooting spatial distributions. Geoderma 90, 307–326.
Pierret, A., Capowiez, I., Belzunces, L., Moran, C.J., 2002. 3D reconstructions and quantification of macropores using X-ray computed tomography and image analysis. Geoderma 2002, 247–271.
Plum, M., Filser, J., 2005. Floods and drought: response of earthworms and potworms (Oligochaeta: Lumbricidae, Enchytraeidae) to hydrological extremes in wet grassland. Pedobiologia 49, 443–453.
R Core Team, 2013. R: A Language and Environment for Statistical Computing. R Foundation for Statistical Computing, Vienna, Austria. http://www.R-project.org/.
Sanchez-de Leon, Y., Lugo-Perez, J., Wise, D.H., Jastrow, J.D., Gonzalez-Meler, M.A., 2014. Aggregate formation and carbon sequestration by earthworms in soil from a temperate forest exposed to elevated atmospheric CO_2: a microcosm experiment. Soil Biol. Biochem. 68, 223–230.
Schmidt, M.W.I., Torn, M.S., Abiven, S., Dittmar, T., Guggenberger, G., Janssens, I.A., Kleber, M., Kögel-Knabner, I., Lehmann, J., Manning, D.A.C., Nannipieri, P., Rasse, D.P., Weiner, S., Trumbore, S.E., 2011. Persistence of soil organic matter as an ecosystem property. Nature 478, 49–56.
Schneider, C.A., Rasband, W.S., Eliceiri, K.W., 2012. NIH image to imageJ: 25 years of image analysis. Nat. Methods 9, 671–675.
Schomburg, A., Verrecchia, E.P., Guenat, C., Brunner, P., Sebag, D., Le Bayon, R.C., 2018a. Rock-Eval pyrolysis discriminates soil aggregates formed by plants and earthworms. Soil Biol. Biochem. 117, 117–124.
Schomburg, A., Schilling, O.S., Guenat, C., Schirmer, M., Le Bayon, R.C., Brunner, P., 2018b. Topsoil structure stability in a restored floodplain: impacts of fluctuating water levels, soil parameters and ecosystem engineers. Sci. Total Environ. 639, 1610–1622.
Schomburg, A., Brunner, P., Turberg, P., Guenat, C., Riaz, M., Le Bayon, R.C., Luster, J., 2019. Pioneer plant *Phalaris arundinacea* and earthworms promote initial soil structure formation despite strong alluvial dynamics in a semi-controlled field experiment. Catena 180, 41–54.
Sebag, D., Disnar, J.R., Guillet, B., Di Giovanni, C., Verrecchia, E.P., Durand, A., 2006. Monitoring organic matter dynamics in soil profiles by Rock-Eval pyrolysis: bulk characterization and quantification of degradation. Eur. J. Soil Sci. 57, 344–355.
Sebag, D., Verrecchia, E.P., Cécillon, L., Adatte, T., Albrecht, R., Aubert, M., Bureau, F., Calleau, G., Copard, Y., Decaëns, T., Disnar, J.-R., Hetényi, M., Nyilas, T., Trombino, L., 2016. Dynamics of soil organic matter based on new Rock-Eval indices. Geoderma 284, 185–203.
Shipitalo, M.J., Protz, R., 1988. Factors influencing the dispersibility of clay in worm casts. J.Am. Soil Sci. Soc. 52, 764–769.
Six, J., Elliott, E.T., Paustian, K., 2000. Soil structure and soil organic matter: II. A normalized stability index and the effect of mineralogy. Soil Sci. Soc. Am. J. 64, 1042–1049.
Six, J., Conant, R.T., Paul, E.A., Paustian, K., 2002. Stabilization mechanisms of soil organic matter: implications for C-saturation of soils. Plant Soil 241, 155–176.
Sollins, P., Hormann, P., Caldwell, B.A., 1996. Stabilization and destabilization of soil organic matter: mechanisms and controls. Geoderma 74, 65–105.
Spiers, G.A., Gagnon, D., Nason, G.E., Packlee, E.C., Lousier, J.D., 1986. Effects and importance of indigenous earthworms on decomposition and nutrient cycling in coastal forest ecosystems. Can. J. For. Res. 16, 983–989.
Tanner, C.C., 2001. Plants as ecosystem engineers in subsurface-flow treatment wetlands. Water Sci. Technol. 44, 9–17.
Thonon, I., Klok, C., 2007. Impact of a changed inundation regime caused by climatic change and floodplain rehabilitation on population viability of earthworms in a lower River Rhine floodplain. Sci. Total Environ. 372, 585–594.
Tisdall, J.M., Oades, J:.M., 1982. Organic matter and water-stable aggregates in soils. J. Soil Sci. 33, 141–163.
Turberg, P., Zeimetz, F., Grondin, Y., Elandoy, C., Buttler, A., 2014. Characterization of structural disturbances in peats by X-ray CT-based density determinations. Eur. J. Soil Sci. 65, 613–624.
Vatan, A., 1967. Manuel de sédimentologie. Technip, Paris.
Vergnes, A., Blouin, M., Muratet, A., Lerch, T.Z., Mendez-Millan, M., Rouelle-Catrez, M., Dubs, F., 2017. Initial conditions during Technosol implementation shape earthworms and ants diversity. Landsc. Urban Plan. 159, 32–41.
Vervoort, R.W., Cattle, S.R., 2003. Linking hydraulic conductivity and tortuosity parameters to pore space geometry and pore-size distribution. J. Hydrol. 272, 36–49.
Vogel, H.J., Cousin, I., Roth, K., 2002. Quantification of pore structure and gas diffusion as function of scale. Eur. J. Soil Sci. 53, 465–473.
Wickham, H., 2009. ggplot2: Elegant Graphics for Data Analysis. Springer-Verlag, New York.
Yavitt, J.B., Fahey, T.J., Sherman, R.E., Groffman, P.M., 2015. Lumbricid earthworm effects on incorporation of root and leaf litter into aggregates in a forest soil, New York State. Biogeochemisty 125, 261–273.
Zaller, J.G., Arnone, J.A., 1999. Earthworm and soil moisture effects on the productivity and structure of grassland communities. Soil Biol. Biochem. 31, 517–523.
Zangerlé, A., Hissler, C., Blouin, M., Lavelle, P., 2014. Near infrared spectroscopy (NIRS) to estimate earthworm cast age. Soil Biol. Biochem. 70, 47–53.